

Laser doping of germanium

T. J. Mahaney^a, A. V. Muravjov^a, M. V. Dolguikh^a, T. A. Winningham^a, R. E. Peale^a, Zhaoxu Tian^b, Sachin Bet^b, Aravinda Kar^b, and M. Klimov^c

^aUniversity of Central Florida, Department of Physics, Orlando, FL 32816

^bUniversity of Central Florida, CREOL, Orlando, FL 32816

^cUniversity of Central Florida, Materials Characterization Facility, Orlando, FL 32826

ABSTRACT

A direct-write pulsed Nd:yttrium-aluminum-garnet laser treatment in an aluminum-containing gas was applied to the polished surface of an undoped Ge wafer. After KOH etching to remove metallic aluminum deposited on the surface, secondary ion mass spectroscopy (SIMS) revealed ~60-200 nm penetration for Al at a concentration of $\sim 10^{17} \text{ cm}^{-3}$. Atomic force microscopy showed that surface roughness is much less than the measured penetration depth. Laser doping of Ge is a potential low cost, selective-area, and compact method, compared with ion-implantation, for production of high current ohmic contacts in Ge and SiGe opto-electronic devices.

Keywords: laser doping, germanium

1. INTRODUCTION

The motivation for this work is the need for uniform, large area (cm^2), p+ doped Ge surfaces to serve as ohmic contacts on the active crystals in far-infrared p-Ge lasers¹ (Fig. 1). Such contacts must withstand the high-voltage (kV) high-current (kA) excitation requirements of the laser. Poor contacts are characterized by hot spots which quickly grow until the applied electric field becomes non-uniform and the laser action ceases. Sparking at the hot spot can destroy the active crystal. The contacts must also survive thermal cycling between room and liquid helium temperatures, though in our experience this requirement is usually met without difficulty.

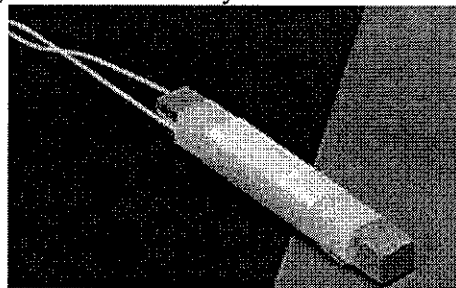


Figure 1 - A p-Ge laser crystal with broad area ohmic contacts and attached leads for high power electrical pulse excitation. The crystal is wrapped in teflon and tape to mechanically support the junction between the wires and the InGa ohmic contacts.

The best ohmic contacts for p-Ge lasers are formed by ion-implantation followed by annealing and evaporation of a gold layer. Wires are readily soldered to such contacts, or connection to the electric-pulse transmission line may be made with springs.² Crystals usually must be sent out for the implantation service, since an ion implanter is major equipment that is rarely handy to the p-Ge laser developer or user. The cost of each implantation treatment is of order \$100, which though significant is small compared to the opportunity cost of the time taken for the service.

Contacts can fail due to handling or accidents, in which case the contacted surface usually must be ground with abrasive to remove possible damage to the crystal. In this process, any implanted layer is lost, and the crystal must to be sent

away again for implantation. It would be more convenient to have a contacting procedure with less equipment overhead and faster turn-around time.

Another method that gives adequate results is coating with an evaporated layer of aluminum followed by annealing at 400 C. Both steps can be combined by using an evaporator with heated sample stage.³ The modest thermal treatment allows some diffusion and activation of the Al acceptor impurity. Indium can be applied to the Al layer afterward to provide mechanical support for wires. A special requirement for this method is that the evaporator should be free from copper parts, which might contaminate the crystal with rapidly diffusing Cu acceptor impurities that can change the laser crystal doping profile in an uncontrolled way. The thermal treatment is confined to temperatures below 400 C precisely to avoid diffusion of this common contaminant. A second issue is that the Al layer must remain clean in order to be wet by indium.

We have adopted some alternate contacting methods, which give less satisfactory results, but which may be used anywhere with a bare minimum of equipment. In one method, indium may be applied directly to the p-Ge laser crystal using an ultrasonic soldering iron.⁴ The ultrasound helps the usually reluctant indium to wet the Ge surface, but there is the possibility that ultrasound introduces microscopic damage which can propagate into the Ge bulk and eventually degrade laser performance. The cost of an ultrasonic iron is of order \$1000. In a second, simpler, cheaper, and currently preferred method, liquid InGa alloy is rubbed on with a toothpick to wet the surface, followed by addition of indium with an ordinary temperature-controlled soldering iron to build up bulk and mechanical strength sufficient to bind the wires. These InGa contacts tend to be mechanically weak, however, and repairs are frequent.

The purpose of this paper is to report initial study of a different surface-doping method which might give a similarly deep p+ layer as ion-implantation but with less equipment overhead. Laser doping⁵⁻⁷ requires a laser, a small vacuum chamber, a gas handling system, and an x-y translation stage. Hence it is similar in complexity to the evaporation scheme, but easier to establish in a small company or university than an ion implanter. The intense short-term localized surface heating in the laser spot up to the melting point promises to achieve deeper diffusion of the p-type dopant than can be achieved by moderate bulk heating at 400 C. Laser doping has been used in SiGe alloys,⁸⁻¹¹ but seems not to have been applied to single crystal germanium before.

2. METHODOLOGY

The starting material for this study was p-type germanium with $>30 \Omega\text{-cm}$ resistivity purchased from University Wafer. This material was determined with a hot probe (see below) to have n-type conductivity. Two $\sim 1 \text{ cm}^2$ pieces were cut from this wafer. These will be referred to as "sample" and "control". The control was irradiated in an Argon atmosphere. The sample was treated in trimethyl aluminum gas. Substitutional aluminum impurities are shallow acceptors in germanium.

A Nd:YAG laser operated at 1064 nm wavelength with a peak power of $\sim 2.6 \text{ kW}$ in a 270 ns pulse at 35 kHz repetition rate to give a duty cycle of $\sim 1 \%$. The sample was mounted in a cell that could be pressurized with flowing gas and which was fitted with a quartz window. The cell was mounted on a motorized x-y translation stage. The polished sample surface was scanned at a rate of 1 mm/s under the beam, which was focused to a 0.25 mm spot to give a peak intensity of 1.3 MW/cm^2 . Thus each point on the treated portion of the crystal received about 8800 laser shots, and the laser spot moved a distance of 30 nm between shots. Several such scans were made side by side to produce $\sim 1 \text{ mm}$ wide laser-treated tracks. Two such tracks were made on the sample at gas pressures of 15 and 30 psi and several were made on the control at similar pressures.

Conductivity type was determined using a hot probe. This consisted of a soldering iron with a sharp clean tip connected in series with a Boonton Electronics Model 95A dual-polarity analog picoammeter and a stainless steel room temperature probe. The cool probe was placed on the semiconductor surface and the hot probe was placed on the surface about 1 mm distant. The magnitude of the thermally induced current was of order microampere. The sign of the deflection of the picoammeter's gauge determines the sign of the majority charge carriers. The sign of the deflection was confirmed using several Ge samples of known conductivity type, both n and p.

Resistivity was estimated using a homemade in-line 4 point probe with stainless steel points separated by ~1 mm on individual torsion springs. A known current I was applied to the outer pins and the voltage drop V was measured on the inner pair. The resistivity was determined according to $\rho = k t V/I$, where k is geometrical correction factor and t is the sample thickness. The method was calibrated on a number of Ge standards of known resistivity.

The sample and control were examined using the CAMECA IMS-3F SIMS Ion Microscope to obtain aluminum concentration maps in regions of their surfaces both laser-treated and untreated. After etching (see below) to remove surface accumulations of metallic aluminum, SIMS depth profiles of the aluminum concentration in the sample were obtained. Aluminum concentration for the sample was calibrated by comparison with a wafer that had been ion implanted with a known dose of aluminum at known energy. Depth calibration was made by measuring the SIMS etch pit with a profilometer.

For removal of metallic aluminum, sample and control were immersed for several minutes in a KOH solution. KOH aggressively attacks aluminum but etches Ge only slowly. The concentration was sufficient to observe evolution of H_2 bubbles, so that complete removal of surface aluminum was judged by cessation of bubble formation. Then the sample was removed, rinsed with water, and allowed to air dry.

A Digital Instruments Nanoscope IIIA atomic force microscope (AFM) was used to image the surface morphology within both laser treated and untreated surface regions. Gross changes in surface morphology were also observed using 45x and 430x optical microscopes. The latter was equipped with a calibrated reticule for determining lateral dimensions.

3. RESULTS

Figure 2 is a schematic of the tracks created by laser treatment of the sample. The shaded regions indicate surface damage that was visible optically. The break in the upper track, labeled "T", is a region of laser treated material that retained the mirror quality of the surface. The labeled regions all correspond to locations where SIMS and AFM data were collected.

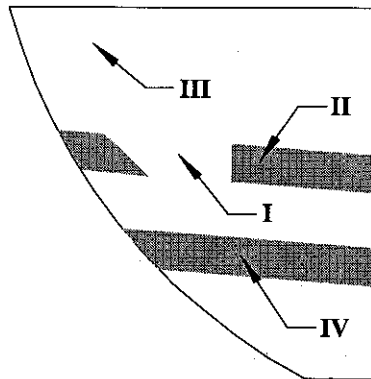


Figure 2 - A schematic of the sample. Visible laser damage is shaded. The labeled areas are regions at which the SIMS and AFM data were taken.

That laser damage was observed on the Ge surface for the given irradiation conditions is understandable. The damage threshold¹² for germanium at our laser pulse duration is of order 1 MW/cm². Our laser intensity was, within likely uncertainties, the same as the damage threshold. The existence of apparently undamaged Region I in the middle of a treated track is evidence that the intensity was for some part of this crystal below the damage threshold. The laser power was constant, which suggests that Region I had a higher damage threshold. The threshold for ablation depends on the defect density,^{13,14} which suggests that Region I has lower defect density. As will be shown, it is only in Region I that Al penetrated can be claimed.

It is interesting that the morphology of the surface damaged regions was different for the sample and control. The sample tracks appear uniformly "frosted" with completely random microstructure. The tracks of the control, on the other hand, display interference colors, and microscope inspection reveals a regular system of parallel grooves at an angle of ~60 deg to the direction of the track. On other parallel tracks, this angle is different. The grooves are separated by a distance of ~12 μm . Such parallel lines on laser damaged Ge have been observed previously using 10.6 μm CO₂ laser radiation.¹⁵ The depth of those features was ~0.5 μm , which is comparable to the characteristic depth of the ablation damage we observe in our sample (see below). The parallel-line pattern was interpreted to result from interference between incident plane waves and spherical waves scattered from surface imperfections, and the lines tended to form parallel to scratches. The spacing of the lines was comparable to the wavelength and could be varied by changing the angle of incidence. In our case, the spacing is greater than the laser wavelength by the factor 11, though the laser beam is normal to the surface. Moreover, the 12 μm period is much greater than the distance moved by the laser spot between shots (29 nm). The ~60 deg angle that the damage lines make with the track is also a puzzle. Hence, the parallel-line damage pattern we observe remains a mystery.

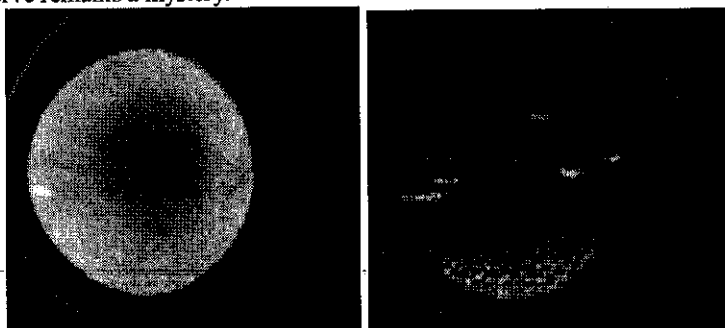


Figure 3 – SIMS aluminum concentration maps within (left) and outside (right) laser treated tracks. The edge of a laser-treated track is visible in the lower part of the right image.

Fig. 3 presents two-dimensional aluminum concentration maps for sample and control surfaces before etching. The highest concentrations are found in the laser treated tracks of the sample, as might be expected. However, spots of high Al concentration appear in the untreated portions of the sample and also on the control. These features suggest that aluminum may splatter outside the laser tracks or that accidental interaction of the laser with Al chamber components may similarly contaminate the surfaces. However these spots of Aluminum cannot penetrate in regions unheated by the laser, and they should be easily removed by KOH etching.

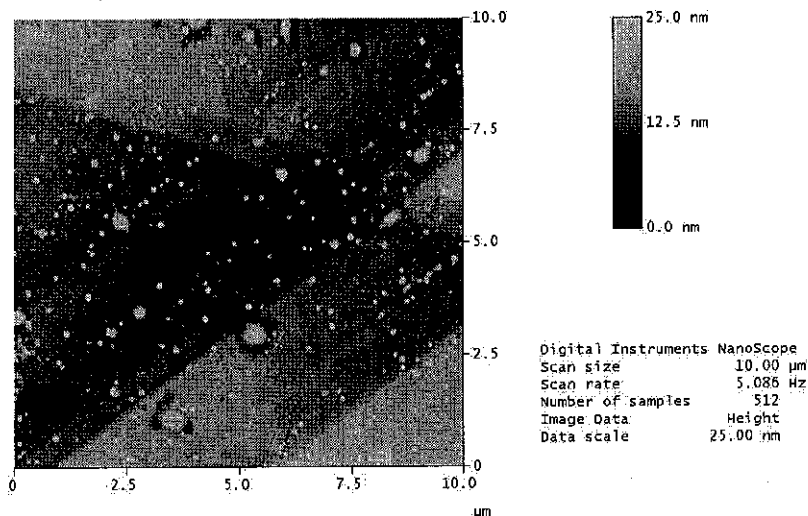


Figure 4 – AFM image of laser-treated region I.

AFM images were collected after etching the sample at points immediately adjacent to the pits created by SIMS measurements (see below). Background Region III of the sample was found to have rms height variations in the range 1 to 2 nm for horizontal scales of 1 to 50 μm , respectively. This roughness is somewhat worse than expected for commercial chemical-mechanically polished epi-ready substrates, which can be attributed to the KOH etch performed by us. Fig. 4 shows that in laser treated Region I the rms roughness is 3 nm on 10 micron horizontal length scales with isolated peaks of order 25 nm in height. In region IV, which has visual evidence of surface damage, the rms roughness exceeds 50 nm and peak-to-peak extremes are as large as 700 nm over horizontal length scales of 10-50 microns.

Figure 5 presents SIMS vertical concentration profiles at several points on the wafer's surface. The location on the sample of each SIMS profile is labeled according to Fig. 2. Usual surface artifacts in SIMS data make these measurements unreliable for depths less than ~ 20 nm. The sensitivity limit for aluminum was about 10^{16} cm^{-3} . Within the untreated background region III, the aluminum concentration is below the sensitivity limit at 20 nm. Two SIMS profiles within region I show an aluminum concentration of 10^{17} cm^{-3} to a depth of 75-200 nm, which exceeds the peak roughness in this region by a factor of 2.4-8. In the damaged regions II and IV, the apparent depth of the aluminum penetration is the same magnitude as the peak surface roughness, so that nothing can be claimed about aluminum penetration in these regions.

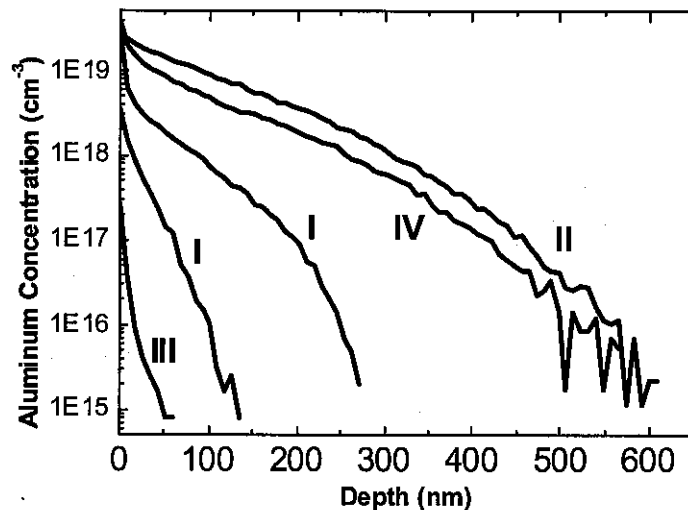


Figure 5 – Vertical aluminum concentration profiles for the regions of the sample indicated in Fig. 1.

Hot-probe tests of the untreated regions and back surfaces of both sample and control reveal n-type conductivity. Tests within all laser treated regions also reveal n-type conductivity. Since p-type conductivity is expected for aluminum doping, hot probe measurements evidently are dominated by the extrinsic conductivity of the nominally undoped substrate. We will return to this point in the discussion section.

Four-point probe measurements on both sample and control gave unexpectedly low sheet resistance, even at untreated points. The resistivity measured in un-treated portions of the sample and control were just a few ohm-cm, i.e. considerably reduced from the 30 ohm-cm value of the starting material. Hence, carrier concentrations throughout the bulk of the sample and control reached levels exceeding 10^{15} cm^{-3} following laser treatment. Extrinsic conductivity of the substrate evidently dominates both hot- and four-point-probe electrical measurements. Possible explanation for the change in substrate resistivity and a proposed solution to allow accurate electrical measurements in laser doped Ge will be discussed in the following section.

4. DISCUSSION

This paper presented initial results of gas-immersion laser-doping of aluminum into Ge. Unambiguous evidence of Al penetration into the Ge bulk to depths of 200 nm was presented. The diffusion coefficient D of Al in crystalline Ge near its melting point is 10^{-13} cm²/s, giving a $\sqrt{(D \tau)}$ diffusion depth of ~ 0.2 nm for a total integrated laser heating time τ of 2.5 ms at a point within a laser-treated track. This consideration is evidence that the surface layer of the sample (in Region I) was at least partly melted by the laser, since impurity diffusion coefficients can be of order 10^8 times higher for liquid phase.⁷

The change in bulk substrate resistivity from >30 ohm-cm to just a few ohm-cm might be explained by bulk heating. The heat capacity of our small sample is only ~ 0.1 J/K while the total energy deposited during a single pass of the laser across its surface is of order 100 J. Hence, neglecting any cooling, the sample temperature would have reached temperatures of ~ 1000 K, i.e. close to the melting point of Ge. Some cooling is of course provided by the flowing pressurized gas and via conduction through the aluminum pedestal on which the Ge sits, but it is easy to imagine that the sample temperature exceeded 400 C, a temperature where certain electrically-active impurities become sufficiently mobile to saturate the sample in remarkably short times. Moreover, oxygen-related thermal donors are generated by annealing in the temperature range 300-450 C.¹⁶ Thus it seems reasonable that bulk heating by the laser changed the conductivity of the substrate. To avoid such effects, Ge samples should be thermally grounded to a cooled substrate in the laser-doping chamber, and the average laser power should be reduced.

It is clearly difficult to characterize the conductivity of an extremely thin doped layer that resides on a thick conducting substrate. Interpretation of four-point probe data for films generally assumes an insulating substrate.¹⁷ Even undoped germanium, with its small (0.67 eV) band gap, has an intrinsic carrier concentration at room temperature of 10^{13} cm⁻³, which in a bulk substrate can short the electrical characterization of highly doped but extremely thin surface layers. Intrinsic conduction may be eliminated by cooling the sample to liquid nitrogen temperature. However, to freeze out extrinsic carriers that originate from shallow dopants, one must cool the sample below 20 K. Fortunately, ultra pure Ge with net electrically-active impurity concentration below 10^{10} cm⁻³, which is used in gamma ray detectors, is available commercially from Perkin Elmer. In future experiments, we plan to use such material and to cool it during electrical characterization.

ACKNOWLEDGMENTS

This work was supported in part by AFOSR contract number F49620-02-C-0027.

REFERENCES

1. T. W. Du Bosq, R. E. Peale, E. W. Nelson, A. V. Muravjov, D. A. Walters, G. Subramanian, K. B. Sundaram, and C. J. Fredricksen, "Wavelength selection for the far-infrared p-Ge laser using etched silicon lamellar gratings," *Optics & Laser Tech* **37**, 87-91 (2004).
2. E. Brundermann, *Long Wavelength Infrared Semiconductor Lasers*, edited by Hong K. Choi (Wiley, NJ, 2004), Chap. 6.
3. A. A. Andronov, I. V. Zverev, V. A. Kozlov, Yu. N. Nozdrin, S. A. Pavlov & V. N. Shastin, *JETP Lett.* **40**, 804 (1984).
4. Eric Nelson, *Gain improvements in p-Ge lasers by neutron transmutation doping*, PhD dissertation, (University of Central Florida, Orlando, 2003).
5. Islam A. Salama, *Laser doping and metallization of wide bandgap materials : SiC, GaN and AlN*, doctoral dissertation, (University of Central Florida, Orlando, 2003).
6. Susan D. Allen, editor, *Laser-Assisted Deposition, Etching, and Doping*, Proc. SPIE **0459** (1984).
7. E. C. Jones, and E. Ishida, "Shallow junction doping technologies for ULSI," *Materials Science and Engineering*, **R24**, 1-80 (1998).
8. S. Krishnan, M. I. Chaudhury, S. V. Babu, "Doping and crystallization of amorphous SiGe films with an Excimer (KrF) laser," *J. Materials Res.* **10**, 1884-1888 (1995).

9. J. Boulmer, C. Guedj, D. Debarre, "Incorporation of substitutional carbon in Si and SiGe by laser processing in methane and propylene," *Thin Solid Films* **294**, 137-140 (1997).
10. A. Slaoui, C. Deng, S. Talwar, J. Kramer, T. W. Sigmon, "Fabrication and doping of poly-SiGe using excimer-laser processing," *Applied Physics A-Materials Science & Processing* **59**, 203-207 (1994).
11. M. Holzmann, P. Baumgartner, C. Engel, J. F. Nützel, and G. Abstreiter, "Fabrication of n- and p-channel in-plane-gate transistors from Si/SiGe/Ge heterostructures by focused laser beam writing," *Appl. Phys. Lett.* **68**, 3025-3027 (1996).
12. J. R. Meyer, M. R. Kruer, and F. J. Bartoli, "Optical heating in semiconductors: Laser damage in Ge, Si, InSb, and GaAs," *J. Appl. Phys.* **51**, 5513-5513 (1980).
13. M. Bertolotti, L. Stagni, G. Vitali, and L. Muzii, Role of Surface Treatment in Laser Damage of Germanium, *J. Appl. Phys.* **42**, 5893-5895 (1971).
14. A. V. Kuanr, S. K. Bansal, and G. P. Srivastava, "Laser-induced damage in InSb at 1.06 μm wavelength - a comparative study with Ge, Si, and Ga As," *Optics & Laser Technology* **28**, 345-353 (1996).
15. D. C. Emmony, R. P. Howson, and L. J. Willis, "Laser mirror damage in germanium at 10.6 μm ," *Appl. Phys. Lett.* **23**, 598-600 (1973).
16. F. Callens, P. Clauws, P. Matthys, E. Boesman, and J. Vennik, "Electron paramagnetic resonance of thermal donors in germanium," *Phys. Rev. B* **39**, 11175-11178 (1989).
17. S. Wolf and R. N. Tauber, *Silicon Processing for the VLSI Era, Volume 1-Process technology* (Lattice Press, Sunset Beach, CA 1986), pp. 119-122.

